TOMSK POLYTECHNIC UNIVERSITY

Available online at www.sciencedirect.com

ScienceDirect

Resource-Efficient Technologies 2 (2016) S177–S185

www.elsevier.com/locate/reffit

Vacuum pyrolysed biochar for soil amendment

Ashish Yadav [a], Khursheed B. Ansari [a], Prithvi Simha [b,c], Vilas G. Gaikar [a], Aniruddha B. Pandit [a,*]

[a] Department of Chemical Engineering, Institute of Chemical Technology, Matunga, Mumbai 19, India

[b] School of Earth, Atmospheric and Environmental Sciences (SEAES), The University of Manchester, M13 9PL, United Kingdom

[c] Department of Energy and Technology, Swedish University of Agricultural Sciences, Box 7032, SE-750 07 Uppsala, Sweden

Received 19 October 2016; received in revised form 1 November 2016; accepted 1 November 2016

Available online 20 December 2016

Abstract

Biochar, a highly carbonaceous charred organic material obtained from biomass conversion can be deliberately applied as a conditioner/amender in order to improve soil quality and associated environmental services. Napier grass (*Pennisetum purpureum*), a lignocellulosic biomass, can potentially be used to produce biochar. The aim of the present work is to manufacture, comprehensively characterize, and apply biochar obtained from the vacuum pyrolysis and investigate its potential for soil amendment. Biochar produced from Napier grass was characterized for its pH, electrical conductivity, soil water retention capacity, surface acidity and/or basicity, elemental composition, Infrared spectra, X-ray diffraction spectra, surface area, porosity, soil–water relation and morphological properties. Experiments on the methylene blue adsorption of the biochar indicated an equilibrium uptake capacity of 35 $mg.g^{-1}$ and showed good agreement with the Langmuir–Freundlich model. Kinetic studies revealed Lagergren pseudo-first-order fit with intra-particle diffusion appearing to be one of the rate controlling mechanisms. Pot trials with *Cicer* grown in neutral and acidic soil amended with biochar validated that biochar augmented plant growth in terms of enhanced biomass weight and number of seed germinations. The entire investigation revealed that the properties of the produced biochar are in line with those necessary for it to act as a suitable agent for soil amendment.

Keywords: Napier grass; Pyrolysis; Biochar; Soil amendment; Adsorption; Crop trials

1. Introduction

Thermo-chemical, bio-chemical and physico-chemical conversion of lignocellulosic biomass represents a coherent renewable source for valuable industrial products [1]. Amongst these processing techniques, thermo-chemical conversion is the fastest and includes vacuum pyrolysis, gasification, and combustion. Vacuum pyrolysis has been extensively used for the conversion of unused biomass and its advantage lies in the process's ability to yield gaseous, liquid and solid products, which is not the case for combustion or gasification. Biochar, a highly carbonaceous charred organic material obtained from biomass pyrolysis, has been deliberately applied as a soil conditioner with the intent of improving soil quality and associated environmental services [2]. Its ability to be a good soil amendment agent lies in its physico-chemical properties, porous morphology, and surface functionalities; these properties, however, are strongly dependent on the operating conditions of the pyrolysis and the nature of the feedstock [3].

Biochar obtained from the pyrolysis of lignocellulosic materials has an expected half-life in the range of 100 to 1000 years, which is approximately 10–1000 times longer than the life times of most soil organic matter. Thus, biochar addition to soil could provide a potential sink for organic carbon [3]. It can also augment pH, plant and microbial growth, nutrient retention, water holding capacity and carbon sequestration in soils while preventing groundwater eutrophication; this, in turn, can reduce fertilizer requirements and environmental deterioration associated with fertilizer use [4–8]. However, prior to soil application, biochar has to be comprehensively characterized since it yields differential effects on different types of soil and/or crops. Furthermore, while the pyrolysis of waste biomass like sugar cane bagasse, pecan shells, bio-solids, household wastes, etc. have been investigated earlier for the production of activated carbon and biochar, their application as a soil amender has received relatively less attention [9–11].

* Corresponding author. Department of Chemical Engineering, Institute of Chemical Technology, Matunga, Mumbai 400019, India. Fax: +91 22 33611020.

E-mail address: ab.pandit@ictmumbai.edu.in (A.B. Pandit).

http://dx.doi.org/10.1016/j.reffit.2016.11.004

Napier grass (*Pennisetum purpureum*), a lignocellulosic biomass, can potentially be used to produce biochar through pyrolysis. The grass undergoes harvesting after 3–4 months of planting and can last up to five years. It is drought-resistant but sometimes may become an aggressive plant that spreads underground and if uncontrolled, can invade crop fields as a weed. Our literature review revealed that, although biomass based biochars have been investigated earlier, Napier grass pyrolysed biochar has not been investigated for soil amendment. Thus, the aim of the present work is to comprehensively characterize as well as utilize biochar produced from Napier grass pyrolysis. Properties investigated include char pH, electrical conductivity, surface acidity and/or basicity, ash and elemental content, surface functionality (infrared spectrocopy), X-ray diffraction spectra, internal surface area, and surface morphology through scanning electron microscopy. Lastly, to evaluate its suitability for soil amendment, the adsorption capacity of the prepared biochar and its effect on plant (*Cicer*) growth were also investigated.

2. Methods and materials

2.1. Materials

Napier grass was obtained from Kirloskar Oil Engines Limited, Pune, India. Initially, it was ground in a mixer to obtain particle size in the range of 1–1.5 mm and then oven dried at 378 K for 5 h until constant weight was obtained. After the removal of moisture, 30 g of dried grass was fed into a SS 316 batch reactor for pyrolysis. The reactor was equipped with 1–15 bar range pressure gauge and a temperature indicator with K-type sensor. The grass was pyrolysed at different temperatures up to 873 K with biochar samples obtained at 573, 673, 773, and 873 K, respectively, in separate experiments.

2.2. Characterization

The pH of the biochar was measured by shaking 2 g biochar in 40 cm^3 distilled water and 0.1 M KCl solutions for 30 min [12]. The electrical conductivity (EC) was determined using a Jenway 4510 conductivity meter by shaking 1 g biochar with 20 cm^3 distilled water for 1 h. The elemental composition of the biochar viz., C, N, H, O, and S content, was determined using a Perkin–Elmer 240B Elemental Analyser. Ash content was analysed by heating the produced biochar to 1073 K in a muffle furnace in the presence of oxygen for 6 h. The ash content was estimated as the difference in the weight of the char, before and after heating it.

The surface acidity and/or basicity of the biochar were estimated by using a Metrohm Tiamo Auto-titrator [13]. Briefly, 0.15 g biochar was shaken with 15 cm^3 of 0.1 N NaOH for 30 h, filtered and an aliquot of 5 cm^3 of the NaOH filtrate was transferred to 10 cm^3 of 0.1 N HCl solution that neutralized any un-reacted base; the solution was back-titrated with 0.1 N NaOH. Similarly, for surface basicity, 0.15 g biochar was shaken with 15 cm^3 of a 0.1 N HCl solution for 30 h. Further, the slurry was filtered and an aliquot of 5 cm^3 of HCl filtrate was transferred to 10 cm^3 of a 0.1 N NaOH solution, which neutralized the unreacted acid. The solution was back-titrated with a 0.1 N HCl solution. The base or acid uptake of the biochar was converted to surface acidity or basicity (mmol/g) [14].

The surface functionality of biochar was measured by infrared spectroscopy (IR). To do this, the chars were mixed with KBr (spectrograde; Merck) in a ratio of 1:200 (w/w) and pelletized using a hydraulic press under constant pressure and further analysed using a Bruker/Vertex 80V FTIR spectrophotometer. The IR spectra were recorded at room temperature (298 K) in the region 4000–400 cm^{-1}. The internal surface morphology was studied using a JEOL-JSM-Scanning Electron Microscope (SEM) after coating with platinum. The electric current was 15 mA and the accelerating voltage was 20–30 kV. The XRD spectra of biochar were recorded on D8 Advance Bruker X-ray diffractor at the wave length 1.5406 Å.

The surface area, pore volume and pore size distribution of the biochar were determined with a Micro Meritics ASAP-2020 Surface Area Analyser. The samples were oven-dried at 378 K for 5 h before the BET surface analysis. Approximately 0.2–0.3 g of the sample was first degassed on a HighVac™ system at 373 K for 4 h, then for a minimum of 24 h at 523 K under a pressure varying as 6.5–9.5 Pa_{abs}. The sample was then introduced into a gas adsorption chamber of the surface area analyser to study N_2 sorption at 77 K.

The effect of biochar on soil water retention capacity was determined by adding 1–5% (w/w) biochar into a suspension of soil (20 g) and water (20 cm^3) and shaking it at room temperature for 24 h. Subsequently, the suspension was filtered and the residual weight was accounted for the measurement of the water retention capacity of the soil.

2.3. Biochar adsorption capacity

The adsorption capacity of biochar was studied by investigating its methylene blue (MB) uptake. This was performed by shaking 0.3 g biochar with 300 cm^3 of MB solution (5–60 ppm concentration) in a multi-magnetic stirrer (Biosystem Scientific) for 24 h at 300 K. During the experiments the pH was monitored with a PH-035 (ATC) pH meter. Further, to study the sorption kinetics, 3 cm^3 aliquots were withdrawn at regular intervals, filtered through a 0.45 μm syringe, and its absorbance was measured using UV–visible spectrophotometer at 630 nm. The equilibrium adsorption of MB was evaluated using Eq. 1; here, C_0 and C_t are the initial and final adsorbate concentrations (mg/dm^3), V is the volume of the solution (dm^3), and W (g) is the mass of the biochar used.

$$q_e = \frac{(C_0 - C_t) \times V}{W} \quad (1)$$

2.4. Biochar application in crop growth trials

The application of biochar for plant (*Cicer*) growth was performed at the Institute of Chemical Technology, Mumbai, located at 19°1′4.73 N and 72°, 50′41.15 E with an altitude of 9 m above from sea level. The mean annual maximum and minimum temperatures of the site are 304.2 K and 296.7 K, respectively, with relative humidity varying between 67 and 78%. Further, the mean annual rainfall of the study area is

2146 mm. The plant growth trials were conducted in two sets of experiments. For each set, pots of 0.2 m diameter and 0.2 m height were filled with 2 kg of 0.0001–0.0002 m sieved dry soil. In the first set of experiments, 20 seeds were planted in three different pots, viz., control (contained no biochar), 0.1% w/w biochar pot, and 0.25% w/w biochar pot. In the second set, the soil pH was adjusted to 5.4 using H_2SO_4 and the biochar was added at the same rate as in set 1. For both studies, plant height, number of germinated seeds, and grown weights after drying were monitored. The plants were watered regularly with deionized water.

3. Results and discussions

3.1. Biochar yield and surface morphology

Table 1 illustrates the yields obtained for biochar produced at 573, 673, 773, and 873 K. The biochar yields were found to decrease with an increase in the pyrolysis temperature. This was probably due to the rapid removal of volatiles from precursor at higher temperatures. The surface morphology of the biochar as studied by SEM revealed its irregular geometry and porous surface (Fig. 1(a)), while the XRD spectra were indicative of its amorphous nature since crystalline carbon peaks at $2\theta = 26°$ were absent (Fig. 1(b)). The peaks obtained at $2\theta = 28$, 40, 50 may be due to the presence of metal impurities (Na, Mg, Ca, K) on the biochar surface.

3.2. Elemental analysis and ash content of biochar

The heating values of the biochars are reported in Table 2 and were found to be in the range of 18–23 $MJ.kg^{-1}$. Interestingly, the elemental analysis revealed that the biochar produced from Napier grass was free from sulphur. This is certainly a salient advantage of the biochar pyrolysis investigated in the present study as the process is likely to reduce emissions of harmful gases like SO_x (SO_2 or SO_3) to the environment which can otherwise be generated due to oxidation of sulphur in the precursor at high temperatures. Table 2 also shows that the biochar pyrolysed at 873 K contained the highest C/N ratio. The C/N ratio was lower than those reported elsewhere for pine chip (38.3), pine bark (209.4), and *Eucalyptus deglupta* (144.6) [15,16]. However, C/N ratios greater than 20 result in immobilization of inorganic N by microbial biomass and cause N deficits in plants [17]. Thus, the biochar obtained in the present study is more likely to have good nutrient retention and release for enhanced plant growth. The O/C and H/C ratios indicate the presence of functional groups on the biochar surface which is essential for natural degradability [18]. The O/C ratios of the biochars were in the range of 0.1 to 0.3 indicating their minimum half-life is around 1000 years (O/C < 0.2) [19]. H/C ratios were observed to be between 0.5 and 2 and are in agreement with those reported in literature for biochar pyrolysed from black wattle (0.54), vineyard pruning (0.59), and sugarcane bagasse (0.64) [20].

3.3. Surface area, porosity, and water retention capacity of biochars

The surface area of biochar as measured by BET method and its nitrogen adsorption/desorption isotherms as well as PSD curve are shown in Fig. 2. The surface area (11–27 $m^2.g^{-1}$) and pore volumes were lower than those reported earlier although, for the biochar prepared at 773 K and 873 K both pore volume (0.029–0.047 to 0.029–0.088 $cm^3.g^{-1}$) and diameter (4–8 to 2.05–2.47 nm) were in agreement with literature values (Table 3) [20]. The low surface area could be due to the structural ordering, pore widening and/or coalescence of neighbouring pores during the pyrolysis. Probably, the low rate of removal of volatiles from the biochar surface caused their accumulation in between and/or within the particles resulting in blocked pore entrances and hence, low surface area. Since the porosity of the char is a key attribute that determines soil aeration and hydrology the biochar pyrolysed at 773 K and 873 K were found to be more suitable candidates for soil amendment. Moreover, the influence of biochar addition on soil water retention capacity was investigated through a series of experiments and it was found that the water retention increased linearly with amount of biochar added (Table 4); soil water

Table 1
Biochar yield with respect to pyrolysis temperatures.

Temperature (K)	Biochar yields (% w/w)
573	52
673	45
773	38
873	36

Table 2
Elemental content and heating values of the prepared chars.

Temperature (K)	C	H	N	S	O	C/N[a]	O/C[a]	H/C[a]	Heating value[b] ($MJ.kg^{-1}$)
573	51.3	4.1	2.7	ND	10.0	12.06	0.26	1.76	21.48
673	54.6	3.6	2.9	ND	6.7	11.93	0.17	1.46	22.50
773	58.3	2.6	2.8	ND	3.9	12.87	0.09	0.98	22.81
873	50.2	1.8	2.4	ND	4.7	13.15	0.13	0.81	18.81

[a] Molar ratio.
[b] Heating value ($MJ.kg^{-1}$) = 33.83*C + 144.3*(H–O/8); ND: not detected.

Table 3
Surface area, pore volume, and average pore diameter for biochar pyrolysed at various temperatures.

Temperature (K)	Surface area of biochar ($m^2.g^{-1}$)	Micropore volume ($cm^3.g^{-1}$)	Average pore diameter (nm)
573	11.0	0.0065	23.70
673	17.5	0.0072	16.20
773	21.6	0.0470	8.68
873	26.1	0.0290	4.38

Table 4
Effect of biochar on soil water retention capacity.

Biochar addition (% w/w)	Increase in soil water retention (%)
1	13.60
2	14.10
3	24.25
4	27.80
5	30.55

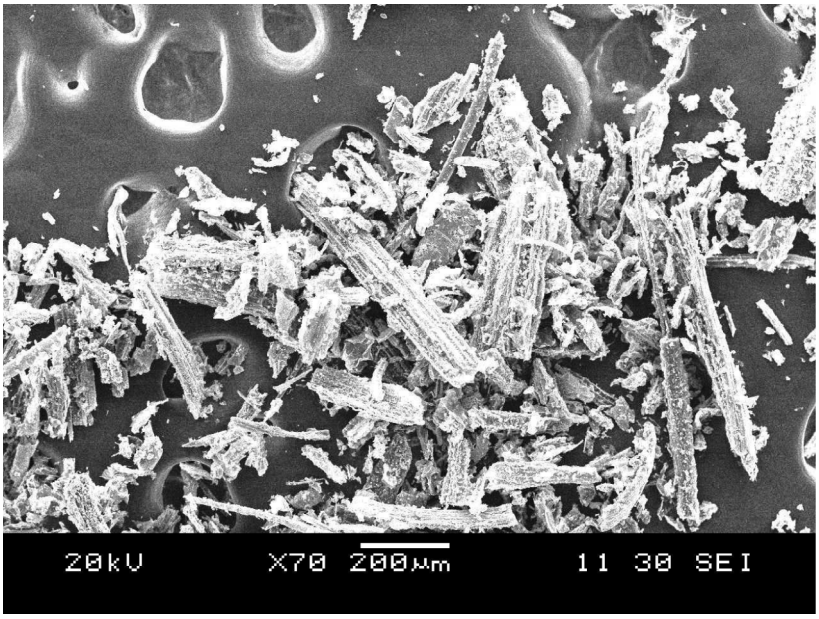

(a)

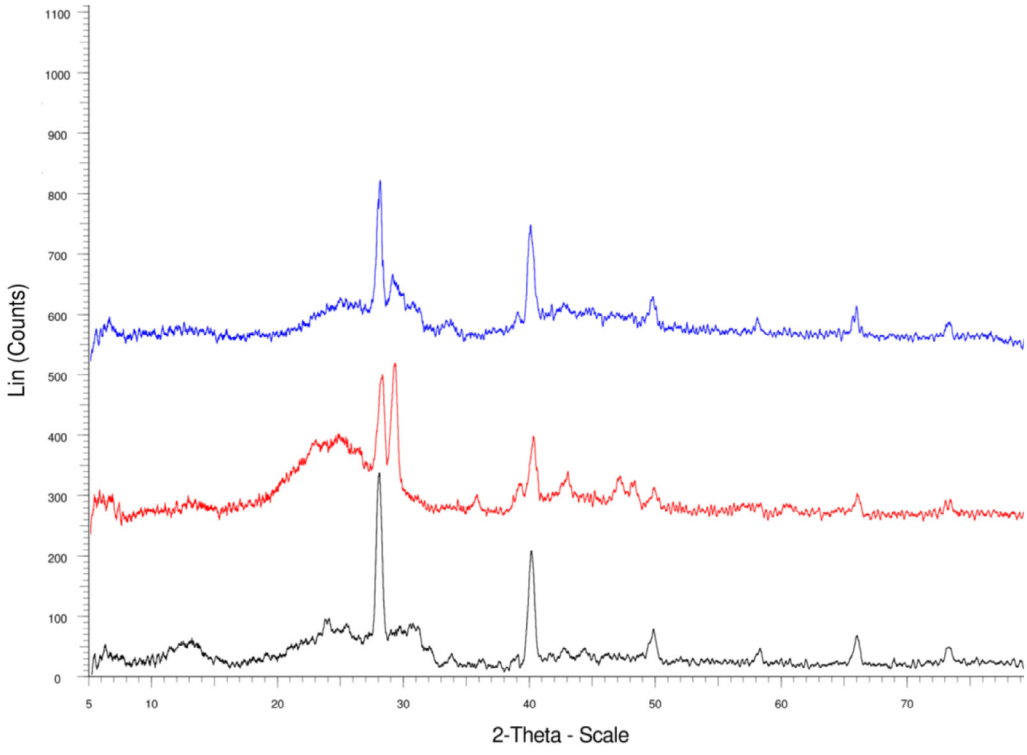

(b)

Fig. 1. (a) SEM image of pyrolysed biochar (b) XRD pattern of biochar at various temperatures (blue: 873 K, red: 773 K, and black: 673 K).

retention capacity increased by 30% with only 5% biochar addition.

3.4. Surface acidity and basicity of biochar

Table 5 reports the surface acidity and basicity of the produced biochars. The surface acidity is apparently caused by the presence of carboxyl, lactones, and phenols (3412 cm^{-1}, and 1616 cm^{-1} peaks in Fig. 3), whereas the presence of carbonates may have contributed to the surface alkalinity (875 cm^{-1} and 803 cm^{-1} peaks in Fig. 3). Table 5 shows that alkaline functionalities of biochars are higher than their acidic functionalities, which is in agreement with biochar obtained from the pyrolysis of vineyard pruning, whereas the reverse has been observed in the case of black wattle and sugarcane bagasse biochar [20]; this indicates that the pyrolysis conditions as well

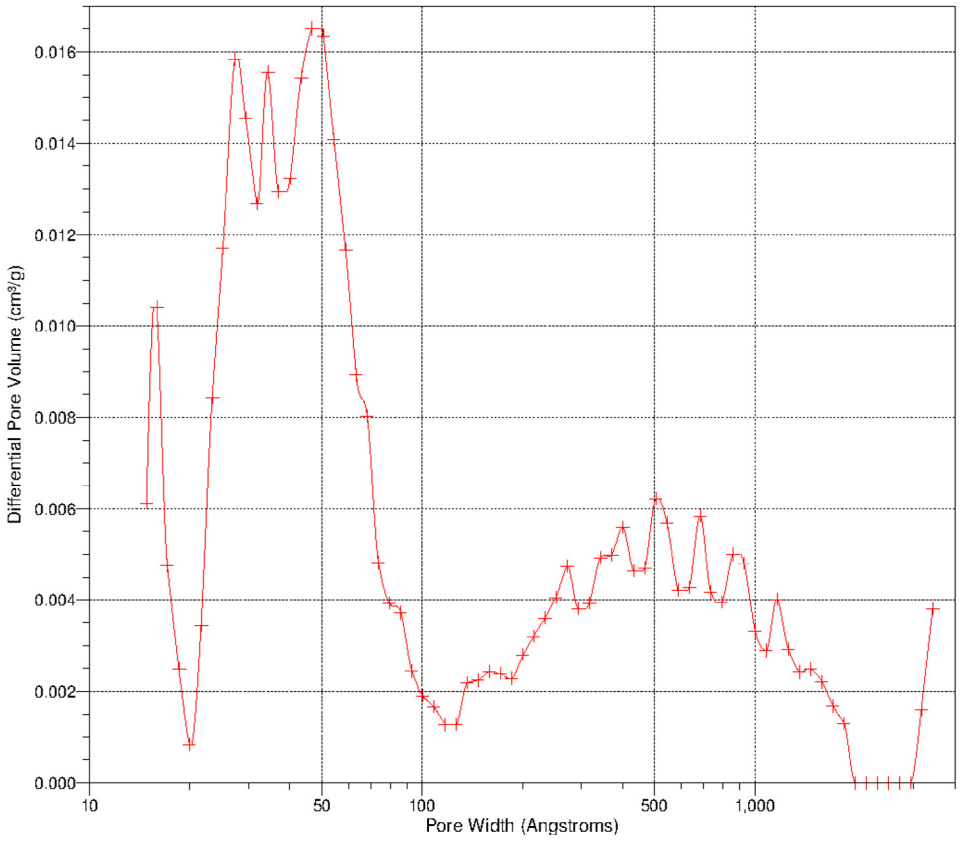

(a)

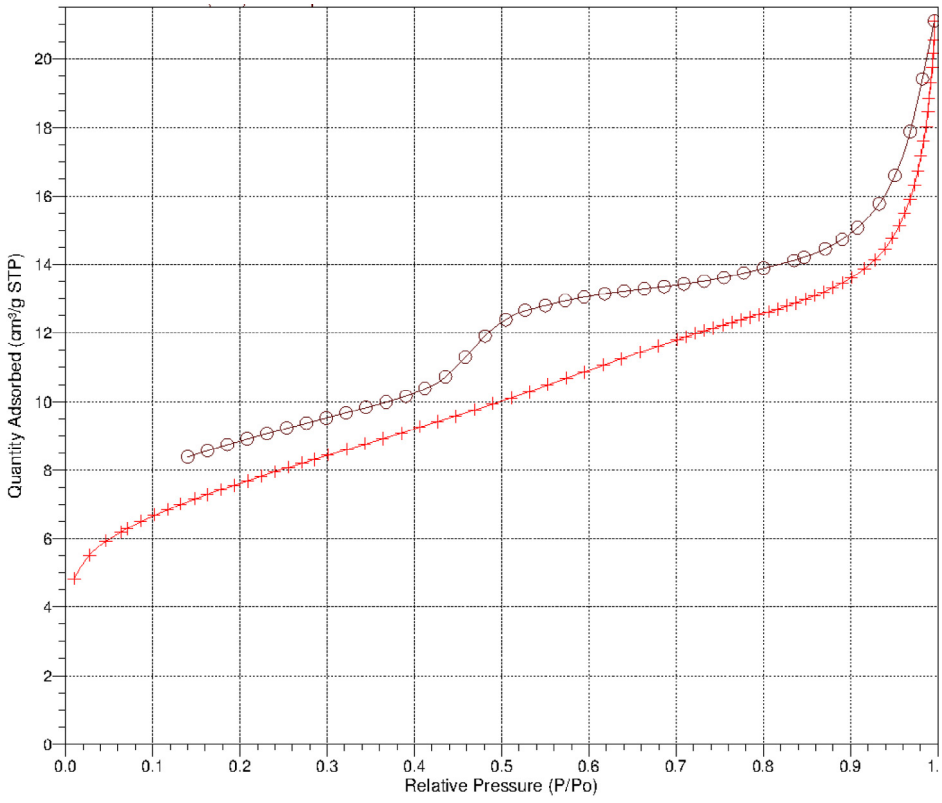

(b)

Fig. 2. (a) Nitrogen adsorption/desorption isotherm and (b) PSD curve for biochar.

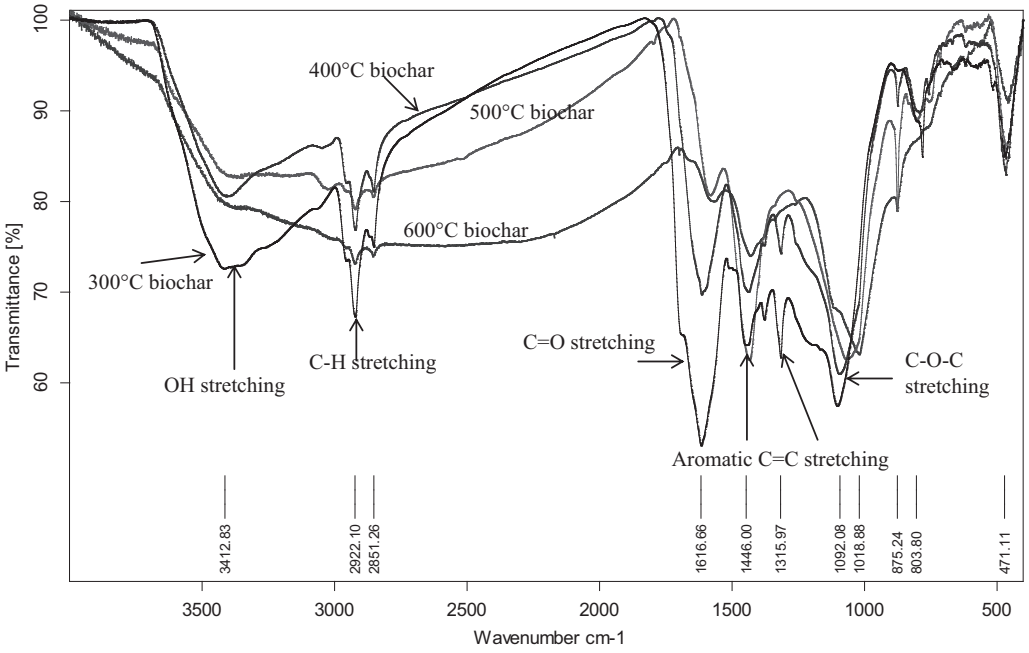

Fig. 3. IR spectra of biochars of Napier grass pyrolysis at various pyrolysis temperatures.

Table 5
Surface acidity and basicity, pH, electrical conductivity (EC), and ash content of the prepared biochars.

Temperature (K)	Surface acidity ($mmol.g^{-1}$)	Surface basicity ($mmol.g^{-1}$)	pH in H_2O	pH in KCl	EC ($dS.m^{-1}$)	Ash content (%)
573	0.088	1.826	8.92	8.38	0.135	20.10
673	0.077	2.155	10.43	9.98	0.156	21.60
773	0.062	2.086	10.56	10.01	0.190	24.22
873	0.055	2.289	11.14	10.87	0.304	25.13

as nature of feedstock have significant effect on the biochar surface functionality. The estimated surface functionalities were also supported by analysis of the IR spectra. Fig. 3 shows that surface of the biochar contained O—H, C—H, C═O, aromatic C═C, CH_2/CH_3, and C—O—C, functional groups. The peaks at 3412 cm^{-1}, 2922 cm^{-1}, and 2851 cm^{-1} are an indication of O—H and C—H functionality. Further, the peaks at 1616 cm^{-1} correspond to C═O stretching of carbonates and lactonic groups of biochars [21], whereas 1446 cm^{-1} peak represents C═C ring stretching for all aromatic biochars and peaks at 1316 cm^{-1} correspond to aliphatic CH_3 deformation. The peaks at 1092 cm^{-1} and 1018 cm^{-1} could be due to aliphatic ether C—O or alcohol C—O stretching [22] while peaks between 875 cm^{-1} and 803 cm^{-1} correspond to carbonates [21].

3.5. pH and electrical conductivity of the biochars

The pH and electrical conductivity of biochar pyrolysed at different temperatures are reported in Table 5. The average difference between pH in H_2O and KCl is 0.45 units indicating a greater amount of exchangeable basicity in the biochars. Further, the biochars showed lower pH in 1 M KCl solution which may be due to their reserve acidity [23]. In soil field, 1 M KCl is used to generate Al^{3+} and H^+ cations to calculate the exchangeable acidity. The generated Al^{3+} and H^+ cations can be easily displaced by K^+ increasing the H^+ concentration in the solution, and consequently decreasing the pH measured in KCl solution. Moreover, Al^{3+} cations of biochars are not exchangeable at pH higher than 5.2 [20]. Usually, the ash content of biochar which mostly comprises metal oxides increases with pyrolysis temperature and this can contribute to the increase in surface alkalinity (Table 5). In general, biochar pH varies from 4 to 13 depending upon the pyrolysis conditions and the nature of the feedstock [24]. However, biochars obtained from most pyrolysis are basic in nature and have a pH in the range of 7.5–9.4 [25]. The electrical conductivity of biochars was observed to increase as a function of the pyrolysis temperature (Table 5). This is indicative of increased salinity which could perhaps be due to the salts of sodium, potassium, magnesium, calcium, and carbonates. Hence, the biochars produced in the present study are likely to increase soil electrical conductivity and it is thus recommended that amount of biochar addition to the soils should be precisely calculated so as to avoid issues like salinization and nutrient imbalances.

3.6. Adsorption capacity of biochars

The initial pH of the MB solution (5–6) increased to around 8–9 due to the addition of biochar and remained in this range throughout the duration of the experiments. Only the adsorption capacity of biochar pyrolysed at 873 K was investigated since it had the highest internal surface area. As seen in Fig. 4(a), the amount of MB adsorbed onto the biochar increased with increase in initial concentration. Initially, the % uptake of MB was high and this is probably due the presence of a large number of vacant sites on the biochar surface However, it remained unchanged after 40 ppm concentration of MB

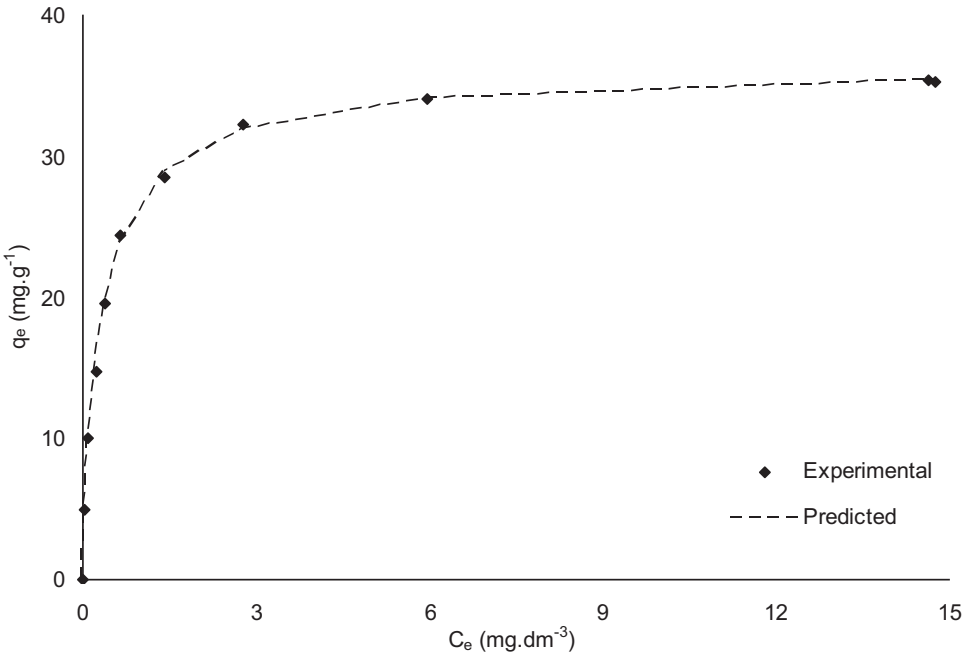

(a)

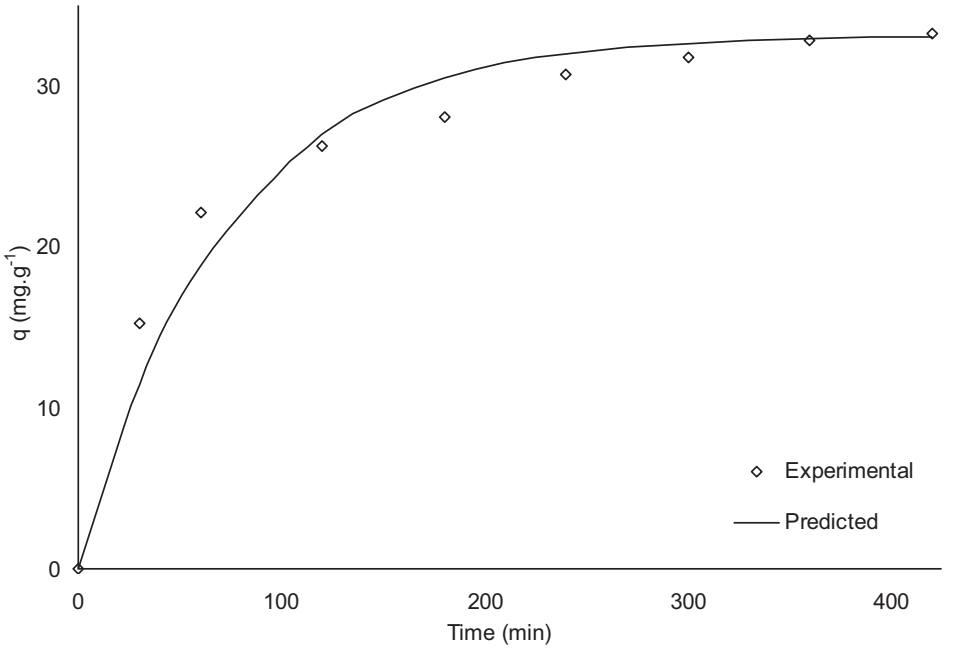

(b)

Fig. 4. (a) Langmuir–Freundlich adsorption adsorption isotherm of methylene blue on biochar. (b) Adsorption kinetics of methylene blue on biochar.

indicating the attainment of an adsorption independent region or saturation of biochar. The adsorption capacity at equilibrium was calculated to be 35 mg.g^{-1} which was lower than literature values for other biochar based adsorbents such as bamboo (319 mg.g^{-1}), rice hull (60 mg.g^{-1}), pine cone (350 mg.g^{-1}), commercial activated carbon (160 mg.g^{-1}), and peach stones (412 mg.g^{-1}) [26]. The lower sorption of MB can be explained by the lower surface area as discussed earlier. Nevertheless, the sorption capacity of the Napier grass biochar was higher than that of rice husk (10 mg.g^{-1}), and was comparable to that of olive stones (38 mg.g^{-1}) [26].

The equilibrium sorption data were also analysed using the Langmuir–Freundlich adsorption model as expressed in Eq. 2 [27]. q (mg.g^{-1}) and Q_m (mg.g^{-1}) are the amount of MB adsorbed at equilibrium and maximum adsorption capacity, respectively, C_e is the equilibrium concentration (mg.dm^{-3}), K_a is adsorption constant (dm^3.mg^{-1}), and n is the index of heterogeneity which usually varies between 0 and 1. For homogeneous surfaces of

materials, n is equal to 1, whereas it is less than 1 for heterogeneous surfaces. Fig. 4(a) shows that a good correlation between the experimental (q_{exp}) and the Langmuir–Freundlich model (q_{predt}) was observed; the maximum adsorption capacity and heterogeneity index values were found to be 36.69 mg.g^{-1} and 0.876, respectively. The heterogeneity in the biochar surface (n < 1) could be due to the presence of various functional groups, as already supported by IR spectra of the biochar (Fig. 3).

$$q_e = \frac{Q_m (K_a C_e)^n}{(K_a C_e)^n + 1} \quad (2)$$

The time required for equilibrium establishment was around 4 h (Fig. 4(b)). Initially, the rate of MB uptake was very high and within 1 h, 90% of MB uptake was completed. The kinetics of methylene blue adsorption on biochar was explained by Lagergren's model as represented in Eq. 3 [28]. K is the rate constant for pseudo-first order adsorption (min^{-1}) and q_e and q_t are the amounts of methylene blue adsorbed (mg.g^{-1}) on the biochar at equilibrium and at time t, respectively. The predicted q_e (33.2 mg.g^{-1}) value was in good agreement with the experimental data (35 mg.g^{-1}) suggesting that the adsorption kinetics is well defined by Lagergren's model.

$$log(q_e - q_t) = log\, q_e - \frac{K}{2.303} t \quad (3)$$

Further, the influence of intra-particle diffusion (Eq. 4) on the adsorption kinetics of Napier grass biochar was observed [29] (figure not shown from brevity). Cross-comparison with literature on MB adsorption indicated that the k_{id} value obtained in the current study (0.143 mmol.g^{-1}.min$^{-0.5}$) was higher than that of activated carbon prepared from *Mimusops elengi* (1.44×10^{-4} mmol.g^{-1}.min$^{-0.5}$) [30], *Morinda coreia Buch.–Ham* (0.0014 mmol.g^{-1}.min$^{-0.5}$) [31], and palm kernel shells (7.52×10^{-4} mmol.g^{-1}.min$^{-0.5}$) [32].

$$ln(q_t) = ln\, k_{id} + 0.5 ln\, t \quad (4)$$

3.7. Effect of biochar on plant growth

In case of neutral soil, the growth of plants in biochar amended soil was faster as compared to the control even though the number of seeds germinated was comparable. The mean heights of the plant on the 20th day in control, 0.1% w/w biochar, and 0.25% w/w biochar amended soils are reported in Table 6; as seen about 20% increase in the plant height in case of biochar amended soil was observed as compared to control. Probably, the addition of biochar influenced soil porosity, pore-size distribution and positively influenced soil–water relations as seen through the high water retention capacity of the produced char [33]; further, as Atkinson et al. (2010) [34] remark, an increase in water retention could potentially extend benefits of improved plant nutrition through mobile soil elements. In comparison to the control, the dried weights of 10 plants from 0.1% w/w and 0.25% w/w biochar amended pots were higher by 18% and 30%, respectively.

In another study, acidic soil with 0% w/w (control), 0.1% w/w, and 0.25% w/w of biochar was seen to have comparable plant heights. However, the number of seed germinations increased with an increase in % biochar addition (Table 6); the number of germinations increased by 35% (at biochar loading of 0.1% w/w) and 57% (at biochar loading of 0.25% w/w), respectively. The acid neutralization effect demonstrated by the biochar is possibly due the presence of carbonates as seen through the IR spectra; for the char pyrolysed at 873 K, the pH (in H_2O) was 11.14 which suggests that biochar addition to acidic soils provides the much necessary pH elevation that, in turn, promotes an enabling environment for plant growth; similar results have been reported by Van Zwieten et al. (2010) [35] for papermill waste biochar. Further, the dried weights of 10 plants from the biochar amended pots were higher by 7% and 15%, respectively, than control.

Table 6
Effect of biochar on plant growth.

Biochar (% w/w)	No. of seeds germinated	Mean plant height (cm)	Dried weight of 10 plants (g)
Neutral soil			
0.00	16	16	4.5
0.10	17	20	5.5
0.25	19	24	6.5
Acidic soil			
0.00	11	14	7.2
0.10	17	15	7.7
0.25	26	15	8.4

4. Conclusions

The biochar produced from pyrolysis of Napier grass was successfully characterized for its various properties. The present study also demonstrated that biochar produced from Napier grass can be applied to acidic soils for their amendment and that it is capable of favourable nutrient and water retention. The adsorption capacity of the produced char indicates that it has good tendency to adsorb toxic compound in the environment. The application of biochar as a soil amender/conditioner in the plant growth trials showed significant effects in terms of increased plant height and enhanced biomass. The entire investigation revealed that the properties of the produced biochar are in line with those necessary for it to act as a suitable agent for soil amendment.

Acknowledgment

Authors KBA and AY would like to acknowledge University Grants Commission India (UGC) and Department of Bioprocess Technology (DBT), respectively, for the financial assistance. KBA and AY are also grateful to IIT-B SAIF, for analytical support.

References

[1] P. McKendry, Energy production from biomass (part 2): conversion technologies, Bioresour. Technol. 83 (2002) 47–54.
[2] J. Lehmann, J. Gaunt, M. Rondon, Bio-char sequestration in terrestrial ecosystems – a review, Mitig. Adapt. Strat. Glob. Change 11 (2006) 395–419.
[3] F. Verheijen, S. Jeffery, A.C. Bastos, M. van der Velde, I. Diafas, Biochar Application to Soils: A Critical Scientific Review of Effects on Soil

Properties, Processes, and Functions, European Commission: Institute for Environment and Sustainability, 2010. http://eusoils.jrc.ec.europa.eu/ESDB_Archive/eusoils_docs/other/EUR24099.pdf. (Accessed 4 March 2012).

[4] A. Downie, A. Crosky, P. Munroe, Physical properties of biochar, in: J. Lehmann, S. Joseph (Eds.), Biochar for Environmental Management: Science and Technology, London, UK and Sterling, 2009.

[5] K.G. Roberts, B.A. Gloy, S. Joseph, N.R. Scott, J. Lehmann, Life cycle assessment of biochar systems: estimating the energetic, economic and climate change potential, Environ. Sci. Technol. 44 (2010) 827–833.

[6] E. Yeboah, P. Ofori, G.W. Quansah, E. Dugan, S. Sohi, Improving soil productivity through biochar amendments to soils, Afr. J. Environ. Sci. Tech. 3 (2009) 34–41.

[7] M.K. Hossain, V. Strezov, K.Y. Chan, P.F. Nelson, Agronomic properties of wastewater sludge biochar and bioavailability of metals in production of cherry tomato (*Lycopersicon esculentum*), Chemosphere 78 (2010) 1167–1171.

[8] P. Simha, A. Yadav, D. Pinjari, A.B. Pandit, On the behaviour, mechanistic modelling and interaction of biochar and crop fertilizers in aqueous solutions, Resour. Effic. Technol. 2 (2016) 133–142.

[9] H. Darmstadt, D. Pantea, L. Summchen, U. Roland, S. Kaliaguine, C. Roy, Surface and bulk chemistry of charcoal obtained by vacuum pyrolysis of bark: influence of feedstock moisture content, J. Anal. Appl. Pyrolysis 53 (2000) 1–17.

[10] P.B. Devnarain, D.R. Arnold, S.B. Davis, Production of activated carbon from South African sugarcane bagasse, Proc. S. Afr. Sug. Technol. Ass. 76 (2002) 477–489.

[11] B.B. Kaudal, D. Chen, D.B. Madhavan, A. Downie, A. Weatherley, An examination of physical and chemical properties of urban biochar for use as growing media substrate, Biomass Bioenergy 84 (2016) 49–58.

[12] M. Carrier, A.G. Hardie, U. Uras, J. Gorgens, J.H. Knoetze, Production of char from vacuum pyrolysis of South–African sugar cane bagasse and its characterization as activated carbon and biochar, J. Anal. Appl. Pyrolysis 96 (2012) 24–32.

[13] H.P. Boehm, Some aspects of the surface chemistry of carbon blacks and other carbons, Carbon 32 (1994) 759–769.

[14] C.H. Cheng, J. Lehmann, Ageing of black carbon along a temperature gradient, Chemosphere 75 (2009) 1021–1027.

[15] M.A. Rondon, J. Lehmann, J. Ramirez, M. Hurtado, Biological nitrogen fixation by common beans (Phaseolus Vulgaris L.) increases with bio–char additions, Biol. Fertil. Soils 43 (2007) 699–708.

[16] J.W. Gaskin, R.A. Speir, K. Harris, K.C. Das, R.D. Lee, L.A. Morris, et al., Effect of peanut hull and pine chip biochar on soil nutrients, corn nutrient status, and yield, Agron. J. 102 (2010) 623–633.

[17] B. Singh, B.P. Singh, A.L. Cowie, Characterization and evaluation of biochars for their application as a soil amendment, Aust. J. Soil Res. 48 (2010) 516–525.

[18] C.M. Preston, M.W.I. Schmidt, Black (pyronegic) carbon: a synthesis of current knowledge and uncertainties with special consideration of boreal regions, Biogeosciences 3 (2006) 397–420.

[19] K.A. Spokas, J.M. Novak, R.T. Venterea, Biochar's role as an alternative n–fertilizer: ammonia capture, Plant Soil 350 (2011) 35–42.

[20] U. Umit, C. Marion, G.H. Ailsa, H.K. Johannes, Physico–chemical characterization of biochars from vacuum pyrolysis of South African agricultural wastes for application as soil amendments, J. Anal. Appl. Pyrolysis 98 (2012) 207–213.

[21] E. Fuente, J.A. Menendez, M.A. Diez, D. Suarez, M.A. Montes-Moran, Infrared spectroscopy of carbon materials: a quantum chemical study of model compounds, J. Phys. Chem. B 107 (2003) 6350–6359.

[22] D. Ozçimen, A. Ersoy-Meriçboyu, Characterization of biochar and bio–oil samples obtained from carbonization of various biomass materials, Renew Energy 35 (2010) 1319–1324.

[23] M.S. Ahmed, M.R. Zamir, A.F.M. Sanaullah, Active acidity, reserve acidity, clay content and cec of some tea soils of Bangladesh, Int. J. Agric. Biol. 8 (2006) 89–96.

[24] K.Y. Chan, L. Van Zwieten, I. Meszaros, A. Downie, S. Joseph, Using poultry litter biochars as soil amendments, Aust. J. Soil Res. 46 (2008) 437–444.

[25] J.F. Novak, W.J. Busscher, D.L. Laird, M. Ahmedna, D.W. Watts, M.A.S. Niandou, Impact of biochar amendment on fertility of a southeastern coastal plain soil, Soil Sci. 174 (2009) 105–112.

[26] U. Umit, Biochar from vacuum pyrolysis of agricultural residues: characterisation and its applications (M.S. thesis), Department of Chemical Engineering, University of Stellenbosch, South Africa, pg. 78, 2011.

[27] P.J. Gautham, T.C. Prabhakar, A modified Langmuir–Freundlich isotherm model for simulating ph–dependent adsorption effects, J. Contam. Hydrol. 129 (2012) 46–53.

[28] M.G. Pillai, P. Simha, A. Gugalia, Recovering urea from human urine by bio-sorption onto microwave activated carbonized coconut shells: equilibrium, kinetics, optimization and field studies, J. Environ. Chem. Eng. 2 (2014) 46–55.

[29] M. Ganesapillai, P. Simha, The rationale for alternative fertilization: equilibrium isotherm, kinetics and mass transfer analysis for urea–nitrogen adsorption from cow urine, Resour. Effic. Technol. 1 (2) (2015) 90–97.

[30] N. Renugadevi, R. Sangeetha, P. Lalitha, Kinetics of the adsorption of methylene blue from an industrial dyeing effluent onto activated carbon prepared from the fruits of *Mimusops Elengi*, Arch. Appl. Sci. Res. 3 (2011) 492–498.

[31] S. Arivoli, M. Hema, S. Parthasarathy, N. Manju, Adsorption dynamics of methylene blue by acid activated carbon, J. Chem. Pharm. Res. 2 (2010) 626–641.

[32] E.S. Abechi, C.E. Gimba, A. Uzairu, J.A. Kagbu, Kinetics of adsorption of methylene blue onto activated carbon prepared from palm kernel shell, Arch. Appl. Sci. Res. 3 (2011) 154–164.

[33] J. Major, C. Steiner, A. Downie, J. Lehmann, Biochar effects on nutrient leaching, Chapter 15, in: J. Lehmann, S. Joseph (Eds.), Biochar for Environmental Management Science and Technology, Earthscan, London, 2009.

[34] C.J. Atkinson, J.D. Fitzgerald, N.A. Hipps, Potential mechanisms for achieving agricultural benefits from biochar application to temperate soils: a review, Plant Soil 337 (2010) 1–18.

[35] L. Van Zwieten, S. Kimber, S. Morris, K.Y. Chan, A. Downie, J. Rust, et al., Effects of biochar from slow pyrolysis of papermill waste on agronomic performance and soil fertility, Plant Soil 327 (2010) 235–246.